

PROCEEDINGS OF SPIE

[SPIDigitalLibrary.org/conference-proceedings-of-spie](https://spiedigitallibrary.org/conference-proceedings-of-spie)

All-optical difference engine for in-process defect inspection for roll-to-roll printed electronics

Xiaobing Feng, Rong Su, Tuomas Happonen, Jian Liu, Richard Leach

Xiaobing Feng, Rong Su, Tuomas Happonen, Jian Liu, Richard Leach, "All-optical difference engine for in-process defect inspection for roll-to-roll printed electronics," Proc. SPIE 11053, Tenth International Symposium on Precision Engineering Measurements and Instrumentation, 1105308 (7 March 2019); doi: 10.1117/12.2511140

SPIE.

Event: 10th International Symposium on Precision Engineering Measurements and Instrumentation (ISPEMI 2018), 2018, Kunming, China

All-optical difference engine for in-process defect inspection for roll-to-roll printed electronics

Xiaobing Feng^{1,*}, Rong Su¹, Tuomas Happonen², Jian Liu³, Richard Leach¹

¹ Manufacturing Metrology Team, Faculty of Engineering, University of Nottingham, Nottingham NG8 1BB, UK

² VTT Technical Research Centre of Finland, P.O. Box 1100, 90571 Oulu, Finland

³ Centre of Ultra-Precision Optoelectronic Instrument Engineering, Harbin Institute of Technology, 92 West Da-Zhi Street, Harbin, 150001, China

ABSTRACT

The increasing capabilities of roll-to-roll (R2R) printing processes present challenges for quality control, requiring in-process inspection of large substrates with high resolution at high speed. In this paper, an all-optical difference engine (AODE) sensor has been developed for in-process defect inspection for R2R printed electronics. The AODE sensor achieves high-speed inspection by utilising the principle of coherent optical subtraction to minimise data processing. The capability of the developed sensor is demonstrated using industrial printed electrical circuitry samples and the sensor is capable of inspecting areas of 4 mm width with a resolution of the order of several micrometres.

Keywords: defect detection; optical sensor; roll-to-roll manufacturing; Fourier optics; spatial filtering

1. INTRODUCTION

Roll-to-roll (R2R) printing is a high-volume manufacturing process and often used to produce large-area electronics on flexible substrates at relatively low cost¹. Various printable materials (e.g. conductor, semiconductor, dielectrics) are deposited over large flexible substrates to form thin electrical circuits². R2R printing technologies include screen printing, slot die coating, gravure printing and flexographic printing, where the speed of printing can be up to 50 m/min². As the number of functional units in a R2R production line is typically high, a fast method to detect defects in-process is necessary to improve the reliability of R2R printed products. Currently, in-process defect inspection of R2R printed electronics is mainly achieved using machine vision cameras, where images of the products are captured and compared to reference images. This method involves image post-processing such as feature extraction and registration with the reference image³. In challenging applications where high-resolution inspection over large substrate areas is needed, multiple machine vision cameras can be deployed in parallel. However, the parallel step incurs significant equipment cost and requires a large amount of data post-processing. In this paper, an all-optical difference engine (AODE) sensor is developed to achieve fast in-process defect inspection on R2R printed electronics with relatively low cost. The working principle of the AODE sensor is based on coherent optical subtraction^{4,5} and a self-referencing strategy. High speed defect detection is achieved by virtually eliminating data post-processing at the software level. A prototype AODE sensor is developed using a digital camera and demonstrated by inspecting defects in industrial printed electrical circuitry samples produced with two different R2R processes. The potential of using a photodiode with the AODE sensor for high speed defect size inspection is also discussed.

Correspondence E-mail: xiaobing.feng@nottingham.ac.uk

2. ALL-OPTICAL DIFFERENCE ENGINE

2.1 Coherent optical subtraction

The principle of the AODE is based on coherent optical subtraction, as illustrated in Figure 1. Two objects with the transmission functions g_A and g_B that are positioned side by side are illuminated with coherent light and imaged with a 4f-system. A one-dimensional amplitude grating is placed at the focal plane of L_1 to perform the spatial filtering. The optical subtraction of g_A and g_B is captured by a photon-sensitive detector, where all the information repeated in both images is nulled. This principle is hereby applied to capture only the difference between a nominal object (e.g. g_A) and a test object (e.g. g_B) to achieve defect detection. The detailed theory of the AODE sensor can be found elsewhere⁶.

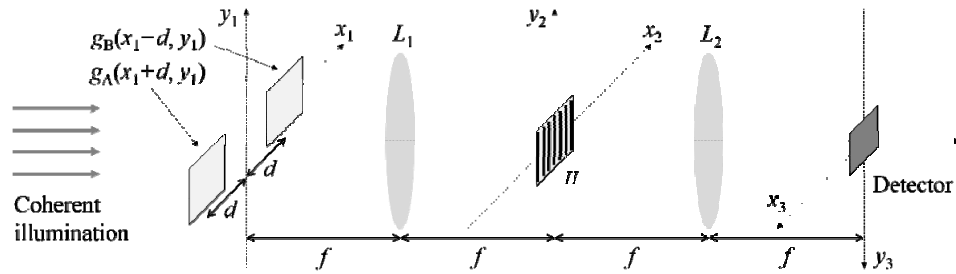


Figure 1. Illustration of the AODE sensor.

2.2 Simulation

Simulation of the AODE is shown in Figure 2. First, the reference object and the test object are defined here as rectangles, with the test object having a square-shaped defect at the centre of the rectangle. The object spectrum is obtained by Fourier transforming the object function. The spatial filter is defined as a sinusoidal amplitude grating. The filtered object spectrum is obtained by multiplying the spatial filter with the object spectrum. The AODE result is then obtained by the Fourier transform of the filtered object spectrum. The defect alone is present in the detection area, as shown in the bottom left image, which corresponds to the peak in the histogram of intensity signal (bottom right) captured by the detector.

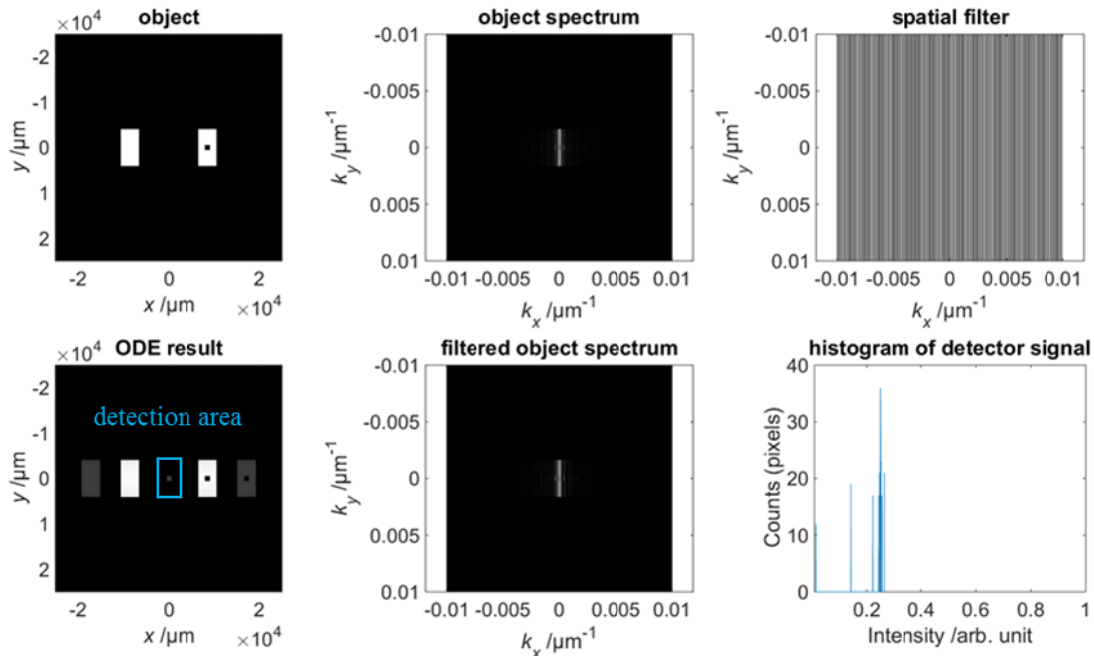


Figure 2. Simulation results of the AODE sensor.

The effect of detector noise is shown in Figure 3, where the defect is an obstacle on the optical transparency. It can be seen that the defect results in an AODE signal peak at the intensity level of around 0.2. This peak gradually disappears when the noise increases, which increases the uncertainty of the defect detection.

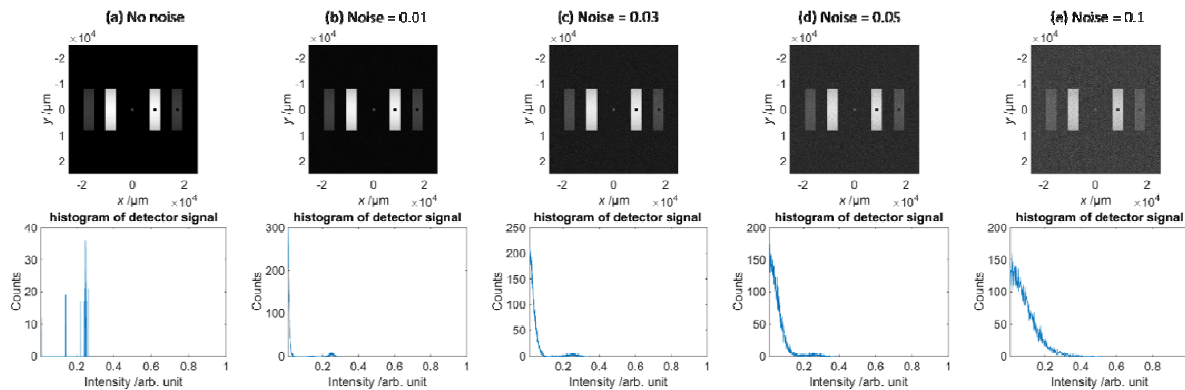


Figure 3. Effect of detector noise on defect inspection. The noise level is normalised to the maximum intensity of the optical transparency.

2.3 Experimental setup

The experimental setup of the developed prototype AODE sensor is shown in Figure 4. The setup consists of illumination, samples and AODE sensor. Specifications of the key optical components in the setup are listed in Table 1.

Illumination is provided by a helium-neon laser output with a single mode fibre. The laser beam is collimated by an achromatic lens of 400 mm focal length. The collimated beam (50 mm in diameter) then illuminates the reference object and the test object.

Both objects were positioned by a sample holder, where two rectangular apertures were aligned to the objects to limit illumination within the region of interest. The sample holder was also designed to allow sliding motion of the objects in order to mimic the movement of the objects during in-process inspection. Light that passes through the apertures and the two objects is collected by the AODE sensor.

The AODE sensor consists of i) a 4f imaging system with 75 mm focal length and ii) a Ronchi grating with 5 μm period at the back focal plane of the Fourier transforming lens as the spatial filter. A two-axis translation stage is used to adjust the position of the grating and optimise the phase angle and focus condition. A CMOS camera is used to receive the optical difference image.

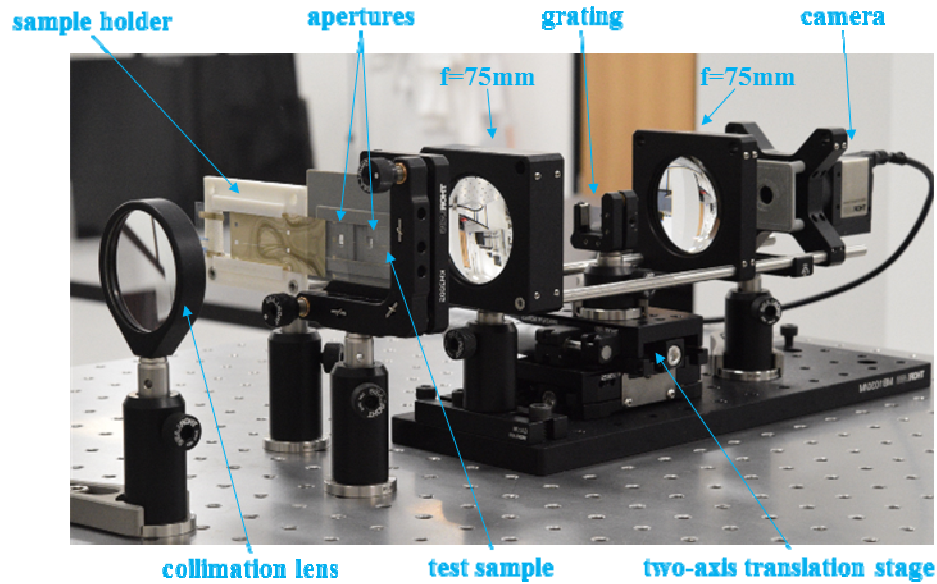


Figure 4. Setup of the AODE sensor. Left: illumination; Right: AODE sensor.

Table 1. Specifications of the optical components in the AODE setup.

Laser wavelength	633 nm	Imaging lens focal length	75 mm
Grating type	Amplitude	Grating period	5 μm
Image sensor pixel size	1280 \times 1024	Image sensor type	CMOS

2.4 Self-referencing strategy

Defect detection by AODE requires a nominal object as the reference. During the R2R process, the printed electronics may be moving at speeds of several metres per minute, which presents the challenge of maintaining precise alignment between the reference and the test object in motion. This challenge can be overcome by a self-referencing inspection strategy which takes advantage of the highly-parallel nature of the R2R manufacturing process. Electronic circuitries printed in R2R processes often consist of continuous and/or repetitive patterns, as shown in Figure 5. Two self-referencing strategies can, therefore, be deployed to use either a different part of a continuous feature, or use a nearby repetitive feature, as the reference, as illustrated in Figure 6. Adopting the self-referencing strategy eliminates the need for an additional reference object and hence avoids any modification to the R2R hardware required for aligning the reference to the inspected product. Furthermore, measurement accuracy is improved by eliminating errors due to unsynchronised motion between the two objects.

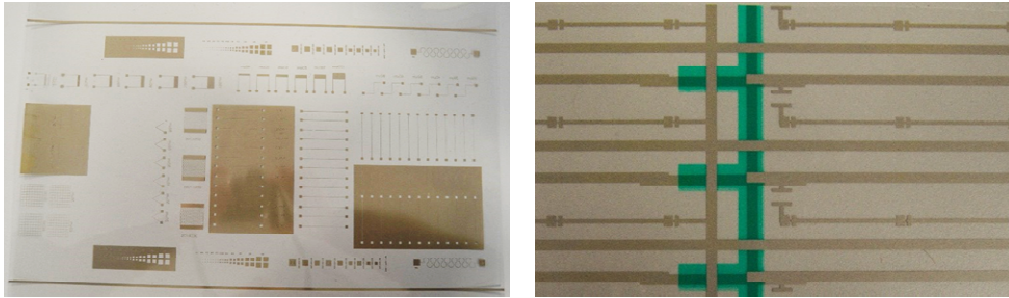


Figure 5. Two examples of electronic circuitries printed by R2R processes.

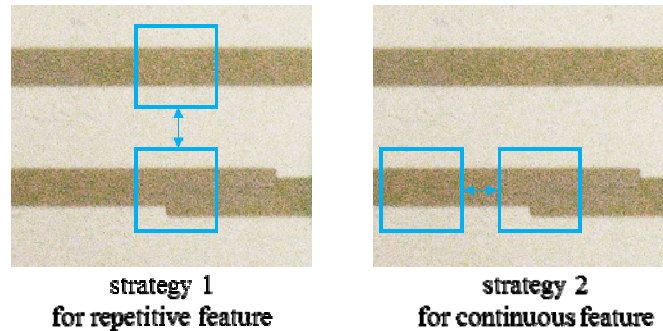


Figure 6. Illustration of the self-referencing strategy. Blue squares represent illuminated fields of view.

2.5 Test samples

Three industrial printed samples, as shown in Figure 7, were inspected for defects to demonstrate the capability of the AODE sensor. The samples were printed with two R2R processes: flexographic printing and rotary screen printing.

Test samples 1 and 2 were R2R manufactured by the flexographic printing method. They were single conductors printed on a 125 μm thick Melinex ST506 PET film with water-based, heat-curable silver nanoparticle ink (PFI-722) from Novacentrix. To demonstrate the capability of the developed inspection system, both samples included artificial manufacturing defects to mimic possible ink transfer failures on the printing plate. The defect on test sample 1 is an incomplete conducting pad, with material missing from a square pad (2 mm nominal dimension). Test sample 2 includes a conducting line (125 μm nominal width) that is missing material for a length of approximately 2 mm.

Test sample 3 is a real application including printed wirings to provide power signals for surface mounted light emitting diodes (LEDs). It was R2R printed by the rotary screen printing method, where the printed patterns were fabricated by squeezing the inks through a screen on the substrate as a non-stop process. The materials used in this sample were heat-treatable Asahi LS-411AW polymer thick film paste, containing micro-sized silver particles, UV-curable Electrodag PF-455 insulator material to form the crossovers, and a 125 μm thick Melinex ST506 PET film as the substrate. As depicted in Figure 7, the printed multilayer structures contained real manufacturing defects due to the misalignment of overlapping conductors. The misalignment width is approximately 0.75 mm. The illustrated defect is typical of multilayer layouts when the separate printing layers are not properly aligned.

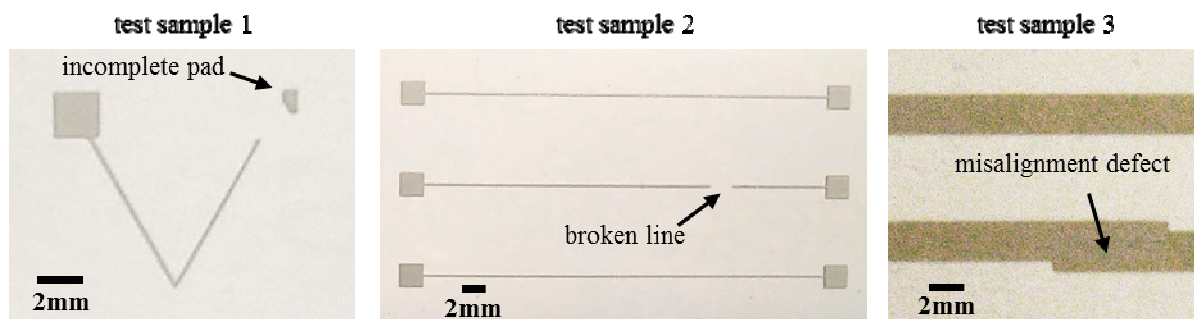


Figure 7. Test samples with various types of defects.

3. RESULTS AND DISCUSSIONS

The captured defects in the three test samples are shown in Figure 8. The reference and object images are illustrated in Figure 8(a)(d)(g), along with the expected difference images. Black areas in the reference and object images indicate the presence of optical obstacles (i.e. ink), while white areas indicate optical transparency (i.e. clear substrate). Any defect will appear bright in the resulting difference images. The difference images captured by the digital camera are shown in Figure 8(b)(e)(h), where detected defects can be seen. A simple intensity threshold can be set at, e.g. 15% of the detector's saturation value, to separate defects from the background. The size of the defects can then be determined from the number of pixels with intensity above the threshold.

In order to estimate the background noise during inspection, difference images were also captured when inspecting high-quality features without discernible defects, which are shown in Figure 8(c)(f)(i). It was observed that background noise could be caused by diffraction (Figure 8(b)(c)), dust particles and scratches on the substrates (Figure 8(e)(f)), and non-uniform thickness of deposited materials (Figure 8(c)(i)). Using the same threshold value, the amplitude of background noise can be determined. The resulting defect-to-noise ratio for the three defects were found to be 56.6, 74.8 and 25.5, respectively.

The developed sensor is capable of inspecting areas of 4 mm width with a resolution of the order of several micrometres.

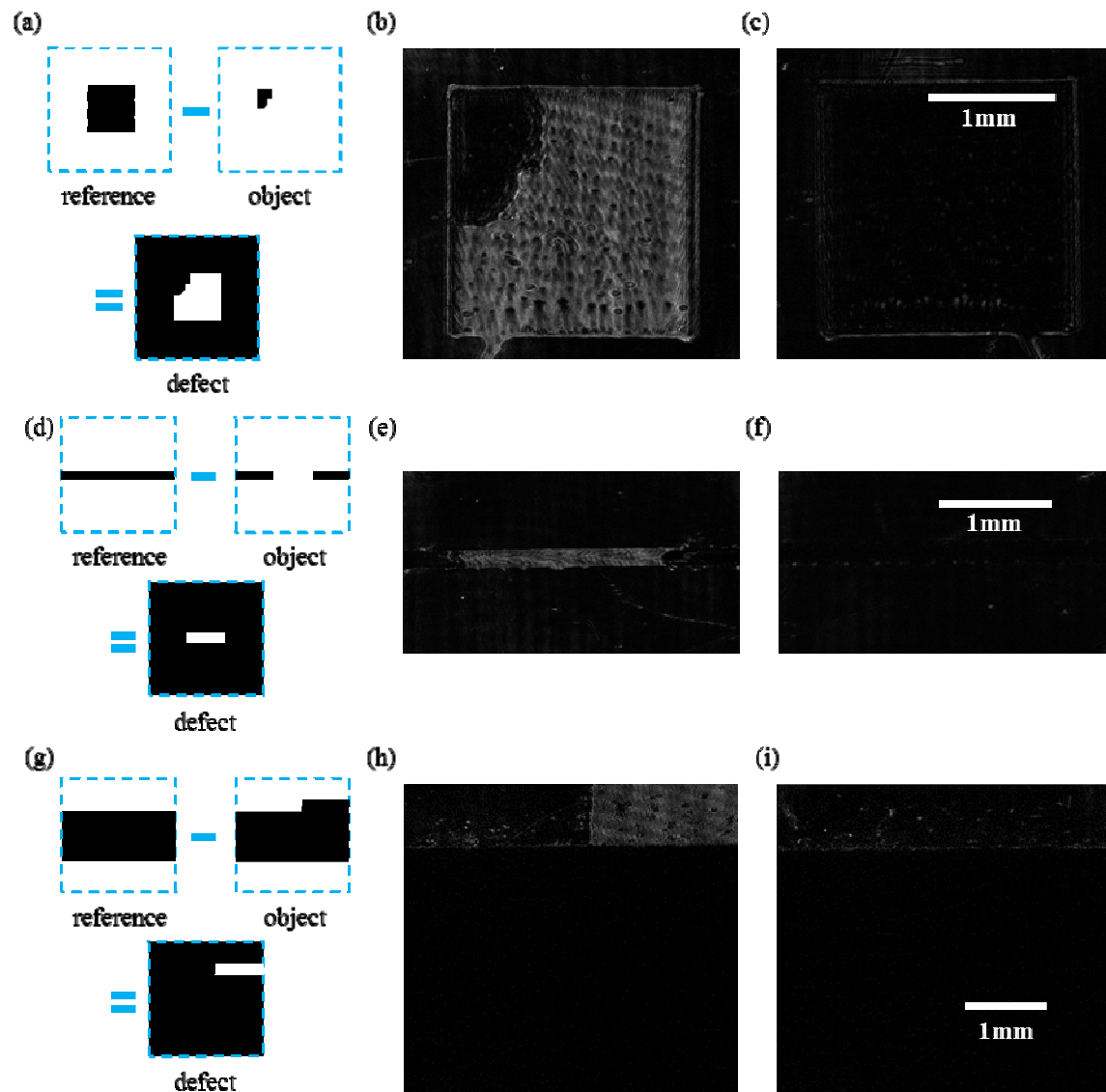


Figure 8. Optical subtraction of test sample 1: (a)(d)(g) illustration of the reference image, the object image and the defect, (b)(e)(h) the difference image showing materials missing from the conducting pad, (c)(f)(i) the difference image when no defect is present.

In order to investigate the effect of substrate misalignment during R2R printing on defect detection capability, a preliminary test was performed where the substrate was moved along the sample holder manually during defect inspection. Figure 9 shows the defect in test sample 2 entering and leaving the detection field of view (FOV), and at different transversal (perpendicular to both web movement direction and optical path) positions. Approximately five degrees of rotation was introduced to the substrate during the movement to illustrate false detection (shown as two parallel lines to each side of the defect in Figure 9) due to rotational misalignment. It is worth noting that in real R2R manufacturing setup, web transversal movement can be controlled with 0.1 mm resolution over several metres length. As a result, rotation misalignment is kept within 0.001° . Therefore, movement of the substrate during R2R printing is well within tolerable limits of the AODE sensor.

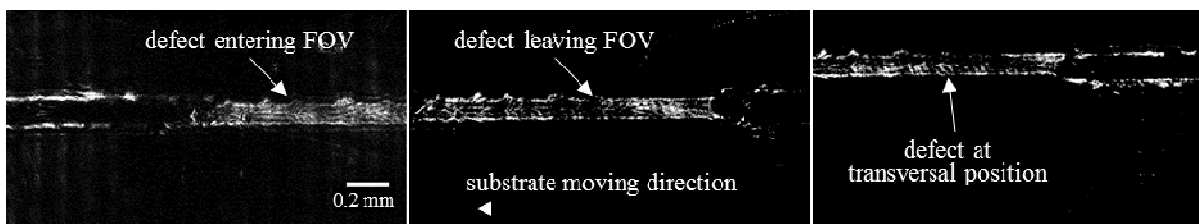


Figure 9. Captured defect in test sample 2 during substrate movement.

In this study, a digital camera was used to capture the difference image in order to illustrate the performance of the AODE sensor. As the total intensity of the detected light directly correlates with the size of the defect, there is no need to perform any advanced signal processing. Therefore, a low-cost photodiode can be used as the detector for defect inspections in situations where only the dimensions of defects is required. A simple photodiode voltage threshold can be set based on a tolerable defect size to make pass-or-reject decisions on-the-fly. In addition, cost-effective parallel sensing system can be built for increasing the total inspection area without compromising lateral resolution.

4. CONCLUSIONS

In this paper, an all-optical difference engine sensor for detecting defects in roll-to-roll printed electronics has been developed. The sensor is based on the principle of coherent optical subtraction and a self-referencing strategy. The performance of the developed sensor was evaluated by inspecting defects on industrial printed electronics samples. The sensor was demonstrated to be able to detect defects down to micrometre level over a field of several millimetres. The self-referencing strategy enables defect detection without an additional physical reference object. Misalignment of the substrate in a typical production line was found to be within tolerable limits of the AODE sensor. Lastly, the use of low-cost gratings, optical fibres for illumination and photodiodes for detection makes it technically and economically more feasible to build parallel inspection systems for in-process pass-or-reject inspection of industrial R2R processes.

FUNDING

This work was supported by European Metrology Programme for Innovation and Research (EMPIR) project MethHPM (14IND09). EMPIR is jointly funded by the EMPIR participating countries within EURAMET and the European Union.

REFERENCES

- [1] Kololuoma, T. K., Tuomikoski, M., Makela, T., Heilmann, J., Haring, T., Kallioinen, J., Hagberg, J., Kettunen, I., Kopola, H. K., "Towards roll-to-roll fabrication of electronics, optics, and optoelectronics for smart and intelligent packaging," *Proc. SPIE* 5363 77-85 (2004).
- [2] Khan, S., Lorenzelli, L., Dahiya, R. S., "Technologies for Printing Sensors and Electronics Over Large Flexible Substrates: A Review," *IEEE SENS. J.* 15(6), 3164-3185 (2015).
- [3] Peng, X., Chen, Y., Yu, W., Zhou, Z., Sun, G., "An online defects inspection method for float glass fabrication based on machine vision," *Int. J. Adv. Manuf. Technol.* 39(11), 1180-1189 (2008).
- [4] Lee, S. H., "Review of coherent optical processing," *Appl. Phys.* 10(3), 203-217 (1976).
- [5] Goodman, J. W., [Introduction to Fourier Optics], W H Freeman: (2005).
- [6] Feng, X., Su, R., Happonen, T., Liu, J., Leach, R., "Fast and cost-effective in-process defect inspection for printed electronics based on coherent optical processing," *Opt. Express* 26(11), 13927-13937 (2018).